

The Major Vault Protein Is a Novel Substrate for the Tyrosine Phosphatase SHP-2 and Scaffold Protein in Epidermal Growth Factor Signaling*

Received for publication, December 22, 2003, and in revised form, May 6, 2004
Published, JBC Papers in Press, May 7, 2004, DOI 10.1074/jbc.M313955200

Sivanagarani Kolli[‡], Christina I. Zito^{‡§}, Marieke H. Mossink[¶], Erik A. C. Wiemer[¶],
and Anton M. Bennett^{‡||}

From the [‡]Department of Pharmacology, Yale University School of Medicine, New Haven, Connecticut 06520-8066 and the [¶]Department of Medical Oncology, Erasmus Medical Center, 3000 DR Rotterdam, The Netherlands

The catalytic activity of the Src homology 2 (SH2) domain-containing tyrosine phosphatase, SHP-2, is required for virtually all of its signaling effects. Elucidating the molecular mechanisms of SHP-2 signaling, therefore, rests upon the identification of its target substrates. In this report, we have used SHP-2 substrate-trapping mutants to identify the major vault protein (MVP) as a putative SHP-2 substrate. MVP is the predominant component of vaults that are cytoplasmic ribonucleoprotein complexes of unknown function. We show that MVP is dephosphorylated by SHP-2 *in vitro* and it forms an enzyme-substrate complex with SHP-2 *in vivo*. In response to epidermal growth factor (EGF), SHP-2 associates via its SH2 domains with tyrosyl-phosphorylated MVP. MVP also interacts with the activated form of the extracellular-regulated kinases (Erks) in response to EGF and a constitutive complex between tyrosyl-phosphorylated MVP, SHP-2, and the Erks was detected in MCF-7 breast cancer cells. Using MVP-deficient fibroblasts, we demonstrate that MVP cooperates with Ras for optimal EGF-induced Elk-1 activation and is required for cell survival. We propose that MVP functions as a novel scaffold protein for both SHP-2 and Erk. The regulation of MVP tyrosyl phosphorylation by SHP-2 may play an important role in cell survival signaling.

are crucial for the regulation of a multitude of physiological processes such as cell growth, differentiation, migration, adhesion, immune response, cell survival, and apoptosis. Although there is overwhelming evidence to demonstrate a critical role for PTPs in the regulation of cellular physiology, a detailed molecular understanding of the actions of many of these enzymes remains to be determined. In large part, the lack of a precise molecular basis for how PTPs function has stemmed from the difficult task of identifying their substrates.

The SH2 domain-containing PTP, SHP-2, is an ubiquitously expressed PTP that has two SH2 domains at the NH₂ terminus, a PTP domain, and a COOH-terminal tail (1–3). Much evidence derived from genetic studies demonstrates that SHP-2 plays a positive role in transducing signals from receptor PTKs (4). Further evidence in mammalian systems for a positive signaling role for SHP-2 has been obtained from mice containing a targeted deletion within exon 3 of murine SHP-2 that deletes the NH₂ terminus SH2 domain (5). SHP-2 exon 3-deleted mice exhibit embryonic lethality (5). Fibroblasts derived from them are defective for the activation of the MAPKs such as the Erks in response to a number of polypeptide growth factors (5–8). These data, as well as those derived from others (9, 10), place SHP-2 upstream of the Erks, and in some cases upstream of either Ras (11), phosphatidylinositol 3-kinase (8, 12, 13) or the Src family kinases (6, 14, 15).

The ability of SHP-2 to transduce downstream signals in such a diverse manner stems, at least in part, from its capacity to participate in a multitude of protein-protein interactions. For example, SHP-2 interacts with scaffolding proteins such as those from the IRS, Gab, and FRS family of proteins (16–19), as well as transmembrane glycoproteins (20–22). These protein-protein interactions often serve to activate SHP-2 through direct engagement of its NH₂-terminal SH2 domain with specific phosphotyrosyl residues (23). In addition, such interactions with SHP-2 also serve to localize it within close proximity to its substrate. Substrates for SHP-2 have been reported previously. For example, the SHP-2 substrate-1, a transmembrane glycoprotein, has been proposed to be a substrate for SHP-2 as well as Gab-1, the EGF receptor, and the signal transducers and activators of transcription (12, 24–26). Despite the identification of these SHP-2 substrates, it is still unclear as to how SHP-2-mediated dephosphorylation propagates positive signaling. Although recently, it has been suggested that SHP-2 signals positively by either negatively regulating GTPase-activating proteins leading to the activation Ras and Rho (27, 28) or through dephosphorylation of the Csk-binding protein resulting in the activation of c-Src (15).

In this report, we describe the identification and functional characterization of MVP as a novel substrate for SHP-2. MVP

Tyrosyl phosphorylation is a dynamic and reversible post-translational modification catalyzed by the opposing actions of PTKs¹ and PTPs. The coordinated actions of PTKs and PTPs

* This work was supported in part by R01-AR46504 and a Burroughs-Wellcome New Investigators Award in the Pharmacological Sciences (to A. M. B.). The costs of publication of this article were defrayed in part by the payment of page charges. This article must therefore be hereby marked "advertisement" in accordance with 18 U.S.C. Section 1734 solely to indicate this fact.

§ Supported by National Institutes of Health Training Grant T32-CA09085.

|| To whom correspondence may be addressed: Yale University School of Medicine, Dept. of Pharmacology, SHM-B 226D, 333 Cedar St., New Haven, CT 06520-8066. Tel.: 203-737-2441; Fax: 203-737-2738; E-mail: anton.bennett@yale.edu.

¹ The abbreviations used are: PTK, protein-tyrosine kinase; EGF, epidermal growth factor; Erks, extracellular-regulated kinases 1 and 2; FRS, fibroblast growth factor receptor substrate; Gab, Grb2-associated binder; GST, glutathione S-transferase; MEF, mouse embryonic fibroblast; IRS, insulin receptor substrate; PTP, protein-tyrosine phosphatase, MAPKs, mitogen-activated protein kinases; MVP, major vault protein; FBS, fetal bovine serum; MALDI-TOF, matrix-assisted laser desorption ionization by time-of-flight mass spectroscopy; PBS, phosphate-buffered saline; FACS, fluorescence-activated cell sorter; JNK, c-Jun NH₂-terminal kinase; GFP, green fluorescent protein.

is conserved evolutionarily and constitutes the predominant component of cytoplasmic ribonucleoprotein complexes called vaults (29–32). The function of the vault organelle remains unknown, although MVP has been found to be overexpressed in many chemoresistant cancer cells and tumors (32). We show that when MVP is tyrosyl-phosphorylated in response to EGF, both SHP-2 and the Erks complex with MVP. MVP also exhibits properties similar to that of other known MAPK scaffold proteins. Our data provide the first functional evidence for MVP as we show that MVP facilitates EGF-dependent transcriptional activation and is required for cell survival.

MATERIALS AND METHODS

Cell Culture—Human WI38 lung fibroblasts and 293 human embryonic kidney fibroblasts were cultured in Dulbecco's modified Eagle's medium containing 10% FBS, 1 mM sodium pyruvate, 50 units/ml penicillin, and 50 μ g/ml streptomycin. MCF-10A cells were a kind gift of Dr. Thimmappaya (Northwestern Medical School, Chicago, IL). These cells were cultured as described previously (33). MCF-7 breast cancer cells were cultured in RPMI 1640 medium containing 10% FBS in the presence of antibiotics. Spontaneously immortalized MEFs were derived from wild type embryos (MVP^{+/+}) and embryos that contained a homozygous deletion of MVP (MVP^{-/-}) (34). The cells were maintained in Dulbecco's modified Eagle's medium and Ham's F-10 at a 1:1 ratio containing 10% FBS, 50 units/ml penicillin, 50 μ g/ml streptomycin, 2 mM glutamine, and 1 mM sodium pyruvate.

Plasmids and Transient Transfections—GST fusion proteins of SHP-2 PTP domain (PTP-WT), PTP domain containing a mutation at Cys⁴⁵⁹ to Ser⁴⁵⁹ (PTP-CS), were generated by PCR amplifying amino acids 218–528 of either wild type SHP-2 or SHP-2 containing a mutation at Cys⁴⁵⁹ to Ser⁴⁵⁹. GST-PTP-DA containing a mutation at Asp⁴²⁵ to Ala⁴²⁵ (PTP-DA) was generated by site-directed mutagenesis using PTP-WT as template. These PTP domain PCR products were subcloned into pGEX-2TK. GST-SHP-2-EA was constructed by PCR amplifying SHP-2-Glu⁷⁶ to Ala⁷⁶ (EA) described previously (35) and subcloning the product into pGEX-2TK. The NH₂-SH2 and COOH-SH2 domains of SHP-2 from amino acids 1–215 (GST-N+C-SH2) have been described previously (36). MVP was cloned into the mammalian vector pcDNA3.1+ (Invitrogen) by reverse transcriptase-PCR using template cDNA isolated from WI38 fibroblasts. WI38-derived cDNA was PCR-amplified using a forward primer that was engineered to contain a HindIII site prior to the start codon (5'-GGATG-AAGCTTACCACCATGGCAACTGAAGAGTTC-3') and a reverse primer containing a KpnI site following the FLAG (DYKDDDDK) tag and a stop codon (5'-GGAGGGTACCTTACTTATCATCATCATCCTTGTAAATCGCG-CAGTAC-3'). The PCR product of the carboxyl-terminal FLAG-tagged MVP was subcloned into pcDNA3.1+ mammalian expression vector using the restriction sites HindIII and KpnI to yield pcDNA3.1-MVP-FLAG (MVP-FLAG). Myc-tagged pIRES-GFP-SHP-2-WT (SHP-2-WT) and pIRES-GFP-SHP-2-C459S (SHP-2-CS) have been previously described (35). pIRES-GFP-SHP-2-D425A (SHP-2-DA) was generated by site-directed mutagenesis using pIRES-GFP-SHP-2-WT as template. All constructs and products generated by PCR were confirmed by DNA sequencing. The vector pDCR and activated H-Ras (pDCR-H-Ras(V12)) were obtained from Dr. Linda VanAelst (Cold Spring Harbor Laboratory, Cold Spring Harbor, NY). 293 cell transient transfections were performed using LipofectAMINE 2000 (Invitrogen) in Opti-MEM (Invitrogen) for 4 h. 293 cells were then placed in complete medium containing 10% FBS for 20 h, prior to serum-deprivation for 24 h. 293 cells were either left unstimulated or stimulated with either 20 or 100 ng/ml EGF (Calbiochem).

Recombinant Protein Expression and Purification of Substrate-trapped Proteins—GST fusion proteins were expressed in *Escherichia coli* and purified as described previously (37). GST-SHP-2 fusion proteins used in the MVP dephosphorylation assay were eluted from the Sepharose matrix by adding 2 bed volumes of the elution buffer (150 mM NaCl, 20 mM Tris-HCl (pH 8.0), 1 mM EDTA, 0.1% Triton X-100, 20 mM glutathione (pH 8.0), and 5 mM dithiothreitol) and incubating for 1 h at 4 °C. SHP-2 substrate-trapped proteins were isolated by large scale affinity purification with GST-PTP-DA from 200 150-mm plates of WI38 fibroblasts. WI38 fibroblasts were first rendered quiescent and then pretreated with 50 μ M pervanadate for 30 min. Cell lysates were prepared in Nonidet P-40 lysis buffer containing 150 mM NaCl, 50 mM Tris-HCl (pH 7.4), 5 mM EDTA, 1% Nonidet P-40, 20 mM NaF, 1 mM benzamidine, 1 mM phenylmethylsulfonyl fluoride, 1 μ g/ml pepstatin A, 5 μ g/ml aprotinin, 5 μ g/ml leupeptin, and 10 mM iodoacetic acid. A total starting yield of ~500 mg of WI38 lysates was isolated which was

subjected to a preclearing step with GST-PTP-WT for 1 h at 4 °C to remove nonspecific PTP interacting proteins. Following preclearing, supernatants were neutralized with 10 mM dithiothreitol and then incubated with GST-PTP-DA for a further 1 h at 4 °C. These affinity complexes were boiled at 95 °C for 5 min in sample buffer and were separated by 8% SDS-polyacrylamide gel electrophoresis (SDS-PAGE). Proteins were visualized by staining with Brilliant Blue-G colloidal stain (Sigma) according to the manufacturer's instructions. Proteins were excised from the polyacrylamide gel, washed in 50% acetonitrile, followed by 50% acetonitrile, 10 mM ammonium bicarbonate. Samples were dried and digested (0.1 μ g/15-mm³ gel) with modified trypsin (Promega) in 10 mM ammonium molybdate. Digested proteins were subjected to matrix-assisted laser desorption/ionization by time of flight mass spectrometry (MALDI-TOF) on a Bruker OmniFLEX™ mass spectrometer (Bruker Daltonics, Inc., Billerica, MA). For vanadate competition experiments, ~10 μ g of GST-SHP-2 fusion proteins were preincubated with 10 mM Na₃VO₄ for 10 min at 4 °C, washed with phosphate-buffered saline (PBS), and then resuspended in PBS prior to use in affinity precipitation experiments. WI38 lysates were incubated with GST fusion proteins for 3 h and washed three times with Nonidet P-40 lysis buffer without iodoacetic acid and then with ST buffer (150 mM NaCl and 50 mM Tris-HCl).

Immunoprecipitation and Immunoblotting—Cells were washed twice in ice-cold PBS and lysed in RIPA buffer (50 mM Tris-HCl (pH 8.0), 150 mM NaCl, 1% Nonidet P-40, 1% sodium deoxycholate, 0.1% SDS, 1 mM EDTA) containing 1 mM phenylmethylsulfonyl fluoride, 1 μ g/ml pepstatin, 5 μ g/ml leupeptin, 5 μ g/ml aprotinin, 10 mM sodium fluoride, 1 mM benzamidine, and 2 mM Na₃VO₄. Cell lysates were used for immunoprecipitation experiments with the respective antibodies for 3 h at 4 °C and then incubated further for 1 h with either protein G- or protein A-Sepharose blocked in 10% bovine serum albumin in PBS. The immune complexes were washed three times in lysis buffer and then once with ST buffer before boiling in sample buffer and separation by 8% SDS-PAGE. Mouse monoclonal anti-MVP (Calbiochem) and anti-FLAG antibodies (Sigma) were used at 0.2 μ g/mg lysates and 2.0 μ g/mg lysates for immunoprecipitating MVP and FLAG-tagged MVP, respectively. Polyclonal antibody to SHP-2 (Santa Cruz Biotechnology) was used at 3 μ g/ml for immunoprecipitation. Tyrosyl-phosphorylated proteins were detected using the monoclonal antibody 4G10 (Upstate Biotechnology Inc.) at a 1:2,000 dilution. Mouse monoclonal anti-LRP/MVP (BD Transduction Laboratories), monoclonal anti-SHP-2 (BD Transduction Laboratories), polyclonal anti-Erk2 (Santa Cruz Biotechnology), and anti-phospho-Erk (Cell Signaling Technology) antibodies were all used at a 1:1,000 dilution for immunoblotting. A rabbit polyclonal anti-MVP antibody that was kindly provided by Dr. Wiemer (Erasmus Medical Center, Rotterdam, Netherlands) was used at a dilution of 1:1,000. Primary antibodies were visualized using enhanced chemiluminescence (Amersham Biosciences) according to the manufacturers instructions using horseradish peroxidase-conjugated secondary antibodies raised against either mouse or rabbit (Amersham Biosciences) at a 1:5,000 dilution.

Elk-1 Transactivation Assays—Cells were co-transfected with the 0.5 μ g of Elk-Gal4, 0.5 μ g of 5X-Gal4-luciferase, and 50 ng of pRL-SV40 *Renilla* for 24 h and serum-deprived for an additional 24 h prior to stimulation with EGF (100 ng/ml) for 4 h. The cells were lysed, and Elk-mediated luciferase and *Renilla* activities were measured using the dual luciferase assay system (Promega).

Confocal Immunofluorescence Microscopy—WI38 fibroblasts were plated onto coverslips and serum-deprived for 24 h. Cells were either left unstimulated or stimulated with EGF (100 ng/ml) for 90 min. Slides were prepared for immunofluorescence as described previously (38). Primary anti-MVP or anti-SHP-2 antibodies were visualized using anti-mouse Alexa fluor 488 and anti-rabbit Alexa fluor 594 (Molecular Probes) secondary antibodies at a dilution of 1:250. Confocal microscopic images were acquired using a C-Apochromat 63 \times /1.2W objective and version 3.2 software on LSM510 META confocal microscope (Zeiss, Germany).

In Vitro MVP Tyrosyl Dephosphorylation—The specific phosphatase activity of GST-SHP-2 fusion proteins were determined using *para*-nitrophenylphosphate as described previously (35). Tyrosyl-phosphorylated MVP was immunoprecipitated from serum-deprived MCF-7 cells lysed in RIPA buffer using anti-MVP antibodies. The immune complexes were first washed in wash buffer (150 mM NaCl, 50 mM Tris-HCl (pH 7.4), 5 mM EDTA, and 1% Nonidet P-40) twice in the presence of phosphatase inhibitors (10 mM NaF and 2 mM Na₃VO₄) followed by two washes in the absence of phosphatase inhibitors. The immune complexes were washed in ST buffer and then once in phosphatase assay buffer (150 mM NaCl, 50 mM Tris-HCl, and 5 mM dithiothreitol). MVP

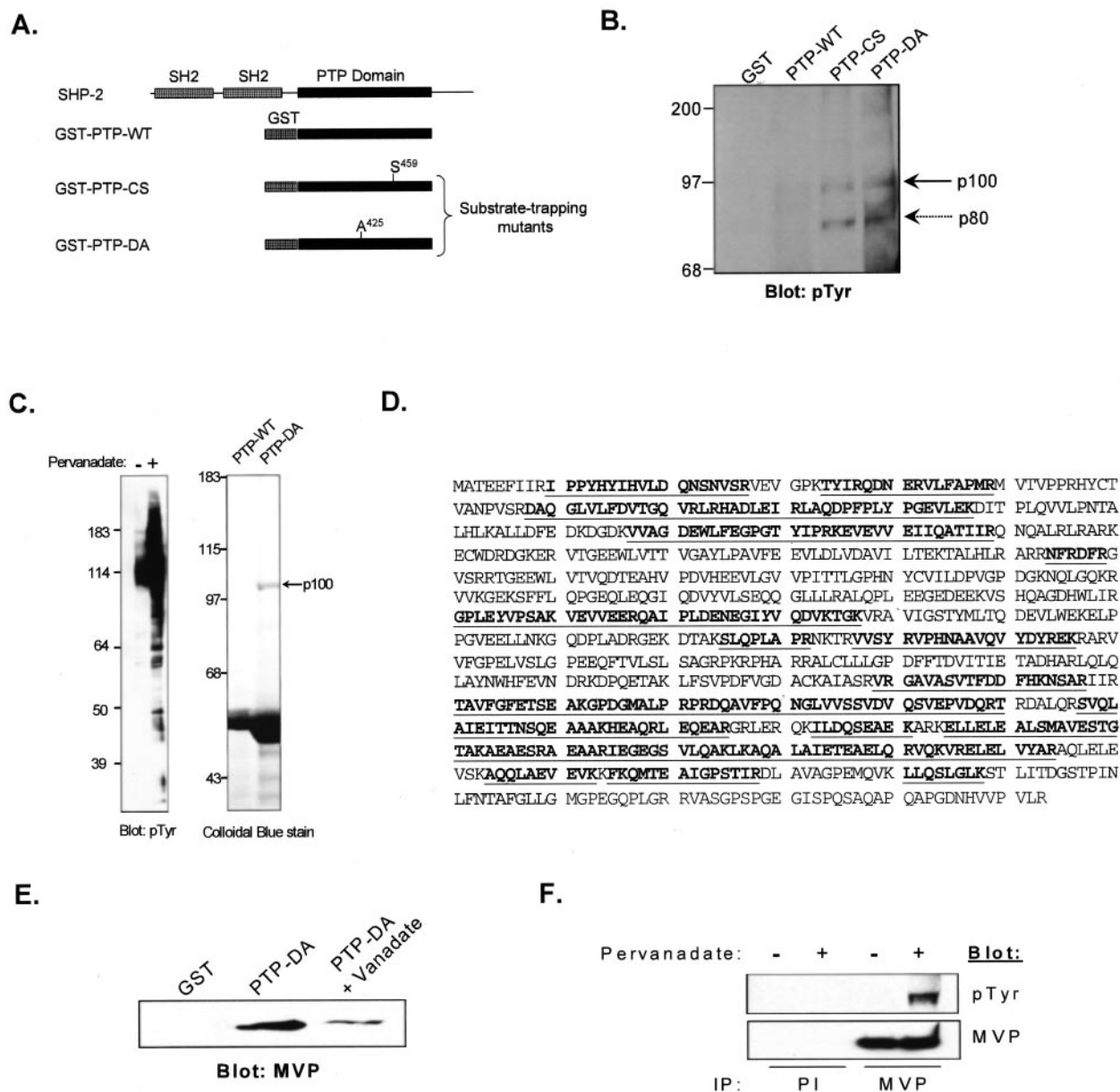


FIG. 1. Identification of a tyrosyl-phosphorylated p100 SHP-2 substrate-trapped protein as MVP. *A*, schematic representation of GST fusion proteins representing wild type (GST-PTP-WT) and substrate-trapping variants (GST-PTP-CS and GST-PTP-DA) of SHP-2. *B*, serum-deprived WI38 cells were pervanadate-treated, and lysates were subjected to affinity precipitation with the indicated GST fusion proteins. Affinity-purified protein complexes were detected by immunoblotting with anti-phosphotyrosine (*pTyr*) antibodies. The arrow at right indicates the substrate-trapped tyrosyl-phosphorylated proteins p100 and p80. *C*, lysates prepared from serum-deprived untreated or pervanadate-treated WI38 cells were resolved by 8% SDS-PAGE and immunoblotted for phosphotyrosine (*left panel*). Colloidal blue staining of SHP-2 substrate-trapped p100 protein (*right panel*). *D*, the excised p100 protein from *C* was subjected to MALDI-TOF spectroscopy, and results were searched against Swiss-Prot. Mass-predicted peptides exhibited a 42.8% match to human MVP. Matched peptides are shown in **bold/underline**. *E*, cell lysates prepared from serum-deprived pervanadate-treated WI38 cells were subjected to GST affinity precipitation with GST-PTP-DA in the absence or presence of vanadate (10 mM). The resulting complexes were resolved and immunoblotted with anti-MVP antibodies. *F*, cell lysates prepared as in *C* were immunoprecipitated with either preimmune (PI) or anti-MVP antibodies. Immune complexes were resolved by SDS-PAGE and immunoblotted for phosphotyrosine (*pTyr*). These immunoblots were re-probed with anti-MVP antibodies.

immune complexes were incubated with equal concentrations of either GST alone, GST-SHP-2-WT, GST-SHP-2-EA, or PTP-WT in the absence or presence of 10 mM Na_3VO_4 at 37 °C for 45 min. The immune complexes were then washed once in the wash buffer containing 10 mM Na_3VO_4 , resolved by 8% SDS-PAGE, and immunoblotted with 4G10 antibodies to detect for the amount of phosphotyrosyl content on MVP. These immunoblots were re-probed to determine the amount of MVP in these immune complexes. Densitometric analysis was performed on tyrosyl-phosphorylated MVP, which was normalized to total MVP ascertained from the re-probe of the immunoblot. Densitometric analysis was performed using Labworks™ analysis software (UVP Inc., Upland, CA).

Cell Death Assays—MVP^{+/+} and MVP^{-/-} MEFs were serum-deprived for different time periods, and both the non-adherent and ad-

herent cells were collected and assessed for trypan blue staining. MVP^{+/+} and MVP^{-/-} MEFs were also subjected to FACS analysis upon propidium iodide staining as described previously (13).

RESULTS

Identification of a Tyrosyl-phosphorylated p100 SHP-2 Substrate-trapped Protein as the MVP—In an attempt to identify substrates for SHP-2, we generated GST fusion proteins encoding the substrate-trapping Cys to Ser (CS) and the Asp to Ala (DA) mutations within the PTP domain of SHP-2 (Fig. 1A). Since SHP-2 contains two SH2 domains, tyrosyl-phosphorylated substrates could potentially interact not only in a SH2-

dependent manner but also via a substrate-trapping interaction. Thus, to ensure that only tyrosyl-phosphorylated substrates were isolated by the substrate-trapping mutants, the SH2 domains of SHP-2 were deleted (Fig. 1A).

The positive role for SHP-2 in growth factor signaling has led to a model in which its substrates undergo tyrosyl dephosphorylation following growth factor stimulation (10). Thus, potential SHP-2 substrates should be tyrosyl-phosphorylated prior to growth factor receptor activation. Therefore, to enrich for these substrates, WI38 human fibroblasts were rendered quiescent and then treated with pervanadate to prevent protein tyrosyl dephosphorylation. Lysates prepared from these cells were incubated with either GST-PTP-WT or substrate-trapping fusion proteins, GST-PTP-CS and GST-PTP-DA (Fig. 1A), and affinity complexes were immunoblotted for phosphotyrosine. We found that whereas GST alone and GST-PTP-WT affinity precipitations exhibited undetectable levels of complexed tyrosyl-phosphorylated proteins, both GST-PTP-CS and GST-PTP-DA fusion proteins precipitated tyrosyl-phosphorylated proteins of 100 kDa (p100) and 80 kDa (p80) (Fig. 1B). Although the p80 protein precipitated with both GST-PTP-CS and GST-PTP-DA, it did so with less efficiency than the p100 protein. Because of this, the p100 protein was selected for further analysis.

To identify the tyrosyl-phosphorylated p100 SHP-2 substrate-trapped protein, we scaled up, by ~60-fold, the affinity precipitation experiment described in Fig. 1B. Fig. 1C (*left panel*) shows the initial repertoire of tyrosyl-phosphorylated proteins present in lysates prepared from quiescent pervanadate-treated WI38 cells prior to affinity purification. These lysates were subjected to affinity precipitation using GST-PTP-WT and GST-PTP-DA. The resultant affinity complexes isolated using GST-PTP-WT and GST-PTP-DA are shown in Fig. 1C (*right panel*). GST-PTP-DA, but not GST-PTP-WT, trapped the p100 protein, which was readily discernable by colloidal blue staining. This p100 protein was isolated and subjected to tryptic digestion followed by MALDI-TOF spectroscopy. The masses of the tryptic digested peptides were queried against the Swiss-Prot database, which returned a match identifying p100 as the human MVP, which also is known as the lung resistance-related protein (Fig. 1D).

If the phosphotyrosyl-containing p100 protein was interacting in a manner dependent upon the formation of an active site intermediate, then this interaction should be disrupted by the PTP catalytic site inhibitor vanadate. To test this and to further confirm that the p100 tyrosyl-phosphorylated protein is indeed MVP, we carried out affinity precipitation assays using either GST-PTP-DA or GST-PTP-DA preincubated with 10 mM vanadate. These affinity complexes were immunoblotted with anti-MVP antibodies. Fig. 1E shows that GST-PTP-DA formed an enzyme-substrate complex with p100, which exhibited immunoreactivity to anti-MVP antibodies. Moreover, the p100/MVP substrate-trapped protein was disrupted from its interaction with GST-PTP-DA by vanadate (Fig. 1E). Although shown to be tyrosyl-phosphorylated in the electric ray (39), no evidence exists as to whether MVP is tyrosyl-phosphorylated in mammalian systems. Therefore, MVP was immunoprecipitated from untreated and pervanadate-treated WI38 cells, and anti-MVP immune complexes were immunoblotted with anti-phosphotyrosine antibodies. As shown in Fig. 1F, MVP was tyrosyl-phosphorylated in pervanadate-treated WI38 cells, consistent with the notion that MVP may serve as a SHP-2 substrate.

SHP-2 Dephosphorylates MVP *in Vitro* and Forms a Substrate-trapped Complex with MVP *in Vivo*—To further characterize MVP as a substrate for SHP-2, we next asked if SHP-2 directly dephosphorylates MVP *in vitro*. GST fusion proteins of

full-length wild type SHP-2 (GST-SHP-2-WT), an activated SHP-2 mutant (GST-SHP-2-EA) (35, 40), and the PTP domain alone (GST-PTP-WT) were generated. The specific activities of these GST proteins were verified using *para*-nitrophenylphosphate as substrate (Fig. 2A). Tyrosyl-phosphorylated MVP was immunoprecipitated from MCF-7 cells and incubated with equal amounts of GST, GST-SHP-2-WT, GST-SHP-2-EA or GST-PTP-WT. Wild type SHP-2 exhibited a low basal level of PTPase activity (Fig. 2A) because it assumes an inactive conformation and thus a minimal effect on tyrosyl dephosphorylation of MVP was observed (Fig. 2B). In contrast, the constitutively active mutant of SHP-2 (GST-SHP-2-EA) that assumes an active conformation independently of SH2 domain engagement exhibited ~10-fold higher levels of PTPase activity than wild type SHP-2 (Fig. 2A) and was capable of dephosphorylating MVP by ~70% relative to GST control (Fig. 2B). Importantly, the ability of GST-SHP-2-EA to dephosphorylate MVP was inhibited by vanadate (Fig. 2B). The PTP domain alone also exhibited high levels of PTPase activity (Fig. 2A) and dephosphorylated MVP completely (Fig. 2B). The PTP domain was also prevented from dephosphorylating MVP by preincubation with vanadate (Fig. 2B). These data provide strong evidence that the catalytic activity of SHP-2 can directly regulate MVP tyrosyl phosphorylation.

To demonstrate that SHP-2 substrate-trapping interactions are not limited to only *in vitro* conditions, we tested whether the substrate-trapping mutants of SHP-2 complexed with MVP within a cellular context. As shown previously (41) the levels of expression of MVP in human WI38 lung fibroblasts are comparatively high relative to HEK 293 cells that express very low to undetectable levels of MVP (Fig. 2C). Thus, 293 cells represent a useful system to study MVP and were used for further experiments. First, FLAG-tagged MVP (MVP-FLAG) was transfected with either the full-length SHP-2 (SHP-2-WT) or the two full-length substrate-trapping mutants of SHP-2 (SHP-2-CS and SHP-2-DA). SHP-2 was immunoprecipitated from lysates prepared from pervanadate-treated 293 cells with anti-SHP-2 antibodies and immunoblotted for the presence of MVP using anti-FLAG antibodies. Ectopically expressed MVP-FLAG in 293 cells complexed with the substrate-trapping mutants, SHP-2-CS and SHP-2-DA; however, no complex formation was detectable with SHP-2-WT (Fig. 2D). The appropriate levels of SHP-2 present in these immunoprecipitates were confirmed by re-probing the FLAG immunoblot with anti-SHP-2 antibodies (Fig. 2D). Collectively, these data demonstrate that SHP-2 binds tyrosyl-phosphorylated MVP via a mechanism that employs direct complex formation with the substrate-trapping mutant of SHP-2 *in vivo*.

MVP Is Tyrosyl-phosphorylated in Response to EGF—If MVP serves as a SHP-2 substrate, we reasoned that MVP might also be a target for tyrosyl phosphorylation in response to growth factors. Therefore, we determined whether MVP is tyrosyl-phosphorylated in response to EGF. Serum-deprived WI38 cells were stimulated with EGF for different times, MVP was immunoprecipitated from lysates prepared from these cells, and immune complexes were immunoblotted for phosphotyrosine. We found that in WI38 fibroblasts, MVP is basally tyrosyl-phosphorylated in serum-deprived cells and is further tyrosyl-phosphorylated upon EGF stimulation by 80–120 min and was subsequently dephosphorylated (Fig. 3A). EGF-induced tyrosyl phosphorylation of MVP was sustained as was the activation of the Erks in these cells (Fig. 3A). When transiently transfected into 293 cells, MVP-FLAG also became tyrosyl-phosphorylated in response to EGF (Fig. 3B). However, the kinetics of MVP-FLAG tyrosyl phosphorylation in response to EGF was more rapid in 293 cells than in WI38 cells (Fig. 3B).

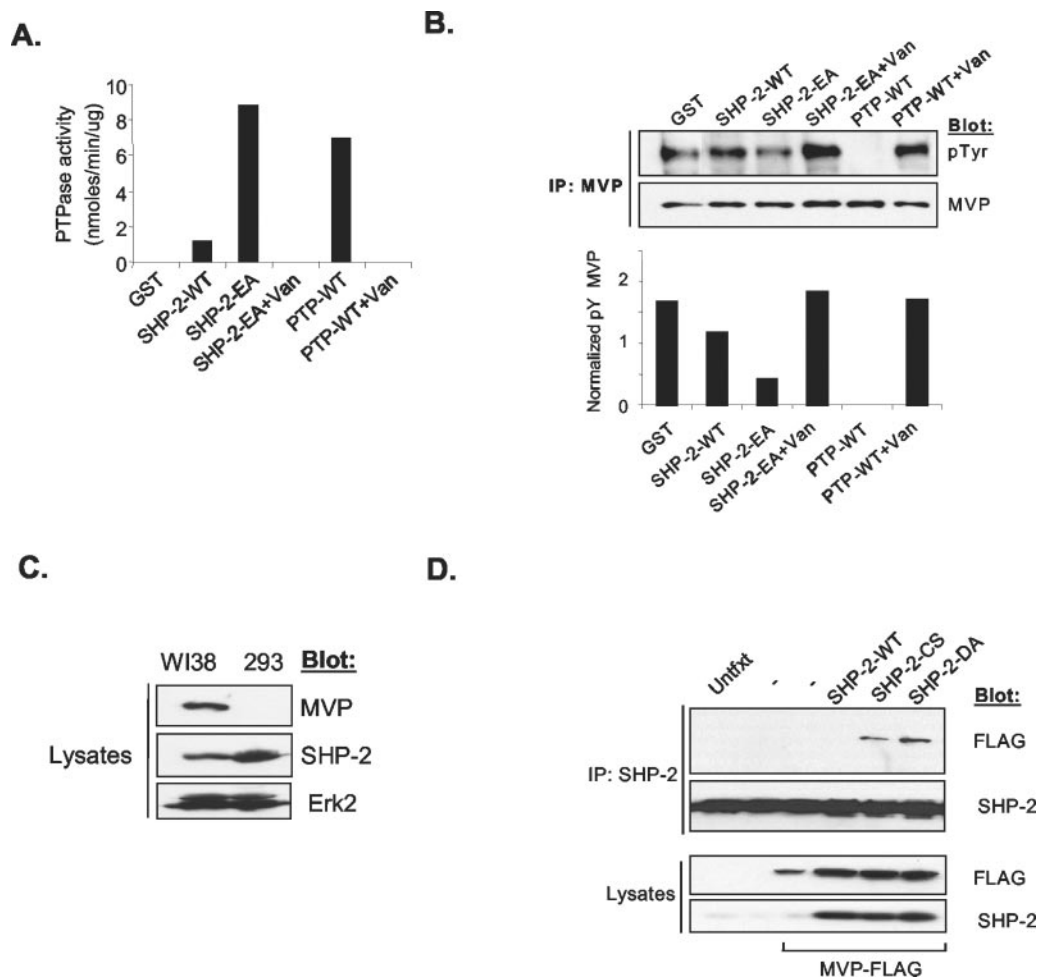


FIG. 2. *In vitro* dephosphorylation and *in vivo* substrate-trapping of MVP by SHP-2. A, GST fusion proteins of SHP-2-WT, SHP-2-EA, and PTP-WT were assayed for PTPase activity using 4 μ g of GST fusion proteins against *para*-nitrophenylphosphate. Where indicated, GST fusion proteins were incubated with 10 mM vanadate (+Van). B, MVP immune complexes after *in vitro* dephosphorylation with the indicated GST fusion proteins were immunoblotted for phosphotyrosine (pTyr). The anti-phosphotyrosine immunoblot was re-probed for MVP. The graph below represents the densitometric analysis of tyrosyl-phosphorylated MVP normalized to MVP from the above experiment. C, expression levels of MVP, SHP-2, and Erk2 in WI38 and 293 cells were determined using anti-MVP, anti-SHP-2, and anti-Erk2 antibodies, respectively. D, 293 cells were co-transfected with MVP-FLAG along with either pIRES-GFP vector (-), SHP-2-WT, SHP-2-CS, or SHP-2-DA. SHP-2 immunoprecipitates from these transfectants were resolved and immunoblotted for MVP using anti-FLAG antibodies. The immunoblots were re-probed with anti-SHP-2 antibodies. Expression levels of MVP-FLAG and SHP-2 in these transfectants were determined by immunoblotting with the indicated antibodies and are shown in the panels labeled as *Lysates*.

Since MVP appears to be tyrosyl-phosphorylated in a growth factor-responsive manner, and the substrate-trapping experiments described previously were carried out under non-physiological conditions using pervanadate, we assessed whether SHP-2 interacted with MVP in a substrate-trapping manner upon EGF stimulation. 293 cells were co-transfected with MVP-FLAG along with either vector control, SHP-2-WT or SHP-2-DA. These cells were serum-deprived for 24 h and then re-stimulated with EGF. SHP-2 was immunoprecipitated using anti-Myc antibodies; immune complexes were resolved and immunoblotted with either anti-phosphotyrosine or anti-FLAG antibodies. Fig. 3C shows that prior to EGF stimulation, SHP-2-DA trapped tyrosyl-phosphorylated MVP. Surprisingly, upon EGF stimulation the SHP-2-DA-MVP complex dissociated (Fig. 3C). These results imply that the putative phosphotyrosyl residue of MVP recognized by the substrate-trapping mutant of SHP-2 exists under physiological conditions prior to stimulation with EGF.

MVP Interacts and Co-localizes with SHP-2 in Response to EGF—In several cases, it has been shown that PTPs interact with their substrates in a non-enzyme-substrate manner. These PTP-substrate complexes presumably facilitate dephos-

phorylation by increasing the relative PTP-substrate concentration. Therefore, we sought to determine whether MVP interacts with SHP-2, in a non-substrate trapping manner as a mechanism to promote MVP dephosphorylation. Cell lysates prepared from unstimulated and EGF-stimulated WI38 cells were subjected to immunoprecipitation with anti-MVP antibodies, and immune complexes were immunoblotted for the detection of SHP-2. Fig. 4A shows that MVP complexed with SHP-2 basally, and this association is enhanced by 90 min after EGF stimulation. In a reciprocal immunoprecipitation experiment, MVP was detected in anti-SHP-2 immune complexes also at 90 min after EGF stimulation (Fig. 4B). The peak level of interaction between SHP-2 and MVP occurred concomitantly with MVP tyrosyl phosphorylation in response to EGF (Fig. 3A). No apparent changes in the total levels of either SHP-2 or MVP were observed during the course of EGF stimulation (Fig. 4C).

To define the region within SHP-2 that interacts with MVP, we generated GST fusion proteins of full-length SHP-2 and the tandem SH2 domains alone. These GST fusion proteins were used to affinity precipitate MVP from pervanadate-treated WI38 cells. As shown in Fig. 4D, not only full-length SHP-2, but

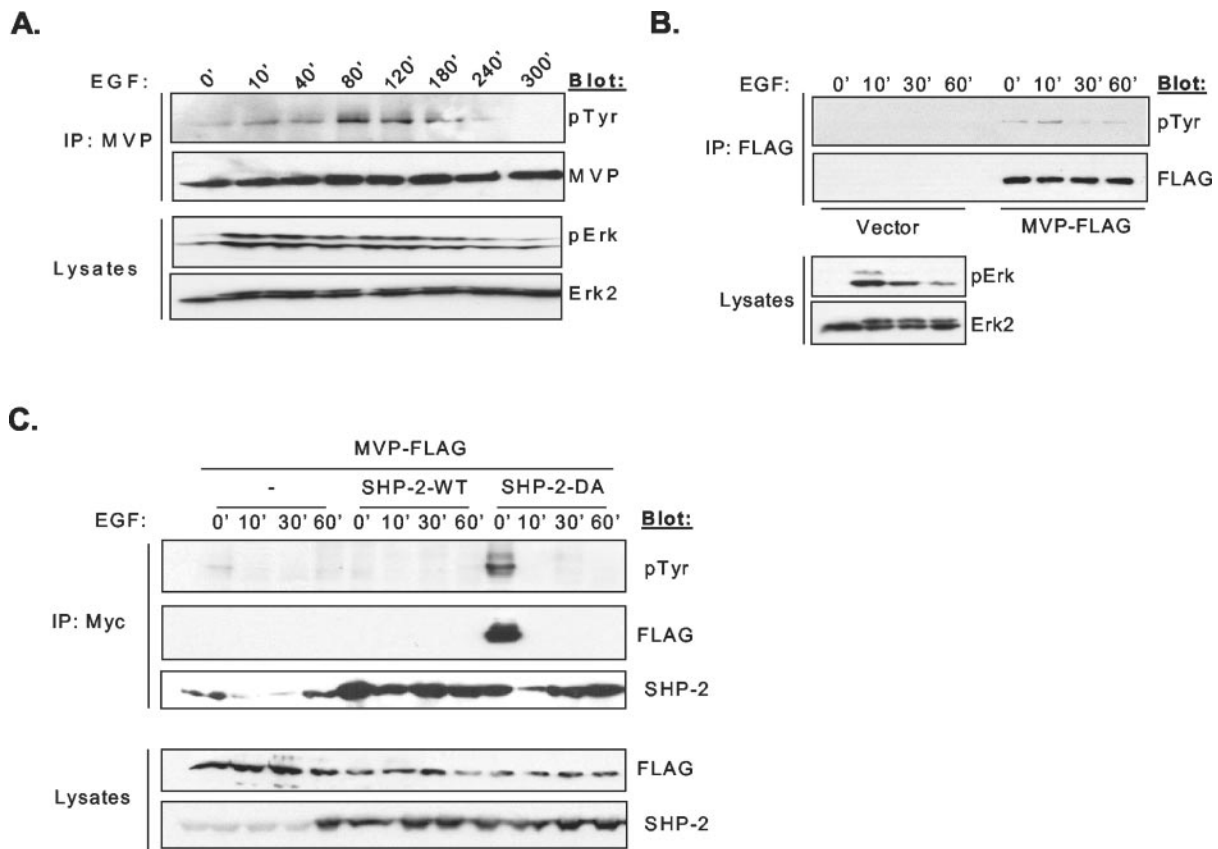


FIG. 3. EGF-dependent tyrosyl phosphorylation of MVP. *A*, serum-deprived WI38 cells were stimulated with EGF (100 ng/ml) for the indicated times. MVP was immunoprecipitated, and immune complexes were resolved by 8% SDS-PAGE and immunoblotted with anti-phosphotyrosine (*pTyr*) antibodies. The phosphotyrosine immunoblots were re-probed with anti-MVP antibodies. Lysates prepared from *A* were immunoblotted with anti-phospho-Erk and Erk2 antibodies. *B*, 293 cells were transiently transfected with either vector control or MVP-FLAG. Serum-deprived 293 cells were either left unstimulated or were stimulated with EGF (100 ng/ml) for the indicated times. Anti-FLAG immune complexes were resolved by SDS-PAGE and immunoblotted for phosphotyrosine (*pTyr*). Levels of MVP-FLAG were determined by re-probing with anti-FLAG antibodies. Erk2 and phospho-Erk levels in these transfectants were determined using anti-Erk2 and anti-phospho-Erk antibodies, respectively. *C*, 293 cells were co-transfected with MVP-FLAG along with either the GFP vector (-), Myc-tagged SHP-2-WT, or SHP-2-DA. These transfectants were serum-deprived and either left unstimulated or re-stimulated with EGF (100 ng/ml). Anti-Myc immunoprecipitates from these cell lysates were resolved and immunoblotted with anti-phosphotyrosine (*pTyr*) and anti-FLAG antibodies. This immunoblot was re-probed for SHP-2 using anti-SHP-2 antibodies. Cell lysates were immunoblotted to confirm for the expression levels of MVP-FLAG and SHP-2 using anti-FLAG and anti-SHP-2 antibodies, respectively (*Lysates*).

also the SH2 domains alone of SHP-2 precipitated MVP. To demonstrate in a more physiological context the observation that the SH2 domains of SHP-2 interacted with tyrosyl-phosphorylated MVP, we transfected MVP-FLAG into 293 cells and determined whether the SH2 domains of SHP-2 associated with MVP in response to EGF stimulation. Fig. 4E shows that upon stimulation with EGF the association of the SH2 domains of SHP-2 with MVP was dramatically enhanced. These data demonstrate that the SH2 domains of SHP-2 mediate the EGF-dependent interaction with tyrosyl-phosphorylated MVP.

To further substantiate the interpretation that MVP complexes with SHP-2, we performed confocal microscopy to detect for co-localization between SHP-2 and MVP prior to and following EGF stimulation of WI38 fibroblasts. We found that SHP-2 was detected in the cytoplasm of WI38 fibroblasts, as expected, but it was detected also in the nucleus (Fig. 4F). SHP-2 has been reported by others to be expressed in the nucleus (25, 42). As published previously (43), MVP was localized to the cytoplasm and, unlike SHP-2, was excluded from the nucleus (Fig. 4F). Upon EGF stimulation, MVP and SHP-2 co-localized (Fig. 4F) at the time point observed when maximal biochemical interactions between them was detected (Fig. 4A). Co-localization between MVP and SHP-2 was not observed in the nucleus. Collectively, these data support the interpretation that SHP-2 complexes with MVP and we identify that SHP-2

can interact with MVP via its SH2 domains.

MVP Complexes with Erk in Response to EGF—Since we had observed that SHP-2 interacts with MVP in an EGF-responsive manner, we surveyed for other potential signaling molecules known to be targets for the EGF pathway that might complex with MVP. In Fig. 5A, we show that when MVP is immunoprecipitated from WI38 fibroblasts, Erk2 is detected in MVP immune complexes between 60 and 90 min following EGF stimulation. It is noteworthy that the association of Erk2 with MVP in response to EGF in WI38 fibroblasts correlated with the kinetics of MVP tyrosyl phosphorylation in these cells (Fig. 3A). We also tested whether both SHP-2 and Erk2 exist in a complex in 293 cells. MVP-FLAG was transfected into 293 cells, and following EGF stimulation, MVP was immunoprecipitated with anti-FLAG antibodies. These immune complexes were immunoblotted for SHP-2 and Erk2. We found that both SHP-2 and Erk2 associated with MVP in a transient manner in 293 cells following EGF stimulation (Fig. 5B). Next, we determined whether the activated form of Erk interacted with MVP in response to EGF by immunoblotting MVP immune complexes with activation-specific phospho-Erk antibodies. When MVP-FLAG was expressed in 293 cells, as shown previously (Fig. 3B), MVP-FLAG became tyrosyl-phosphorylated in response to EGF (Fig. 5C). Although we were able to detect activated Erk in MVP-FLAG immune complexes in the absence of EGF, fol-

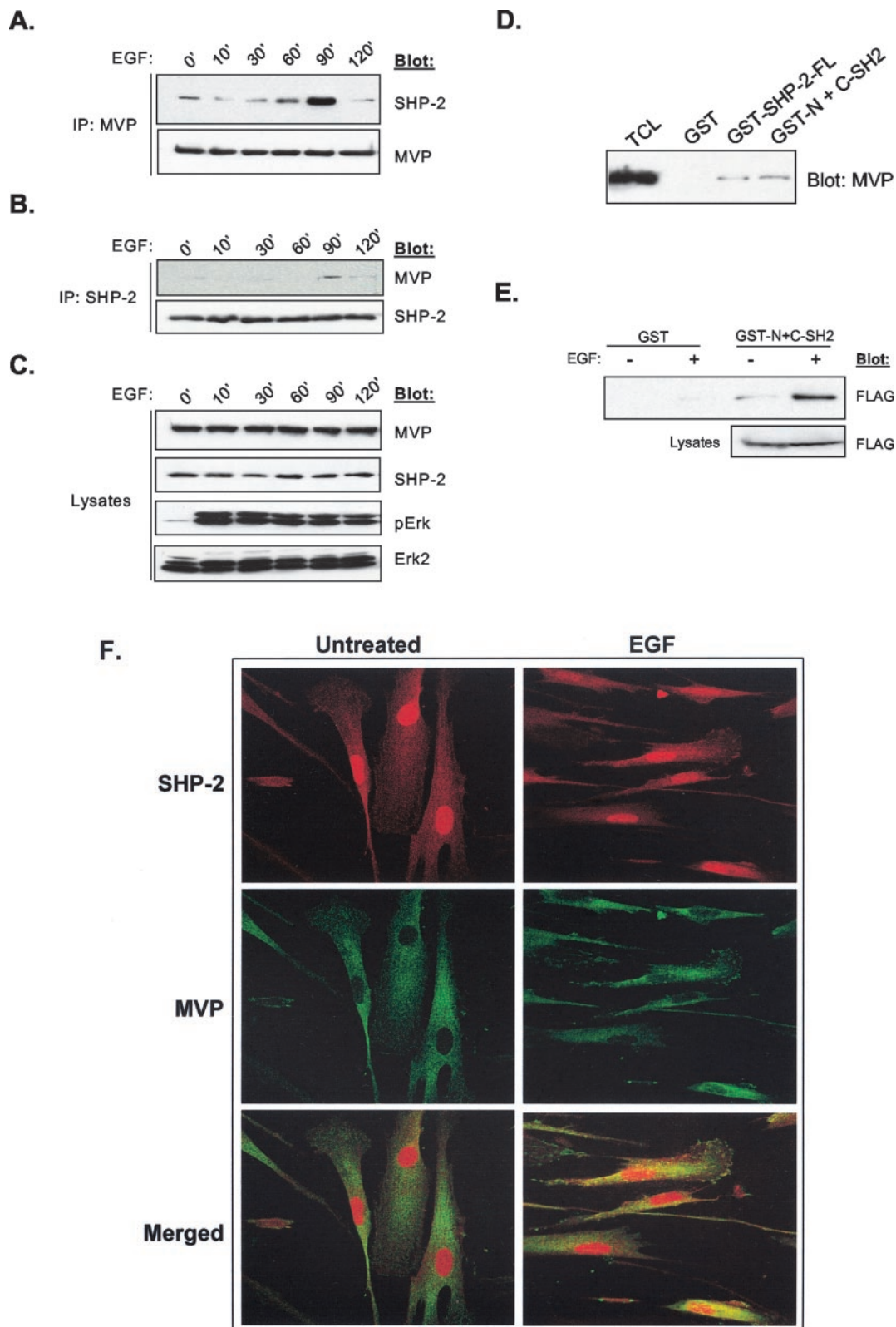


FIG. 4. MVP interacts and co-localizes with SHP-2 in response to EGF. *A*, MVP was immunoprecipitated from serum-deprived and EGF-stimulated (100 ng/ml) WI38 cell lysates and immunoblotted for SHP-2 using anti-SHP-2 antibodies. The SHP-2 immunoblot was re-probed for MVP using anti-MVP antibodies. *B*, SHP-2 was immunoprecipitated from lysates in *A* and immunoblotted for MVP using anti-MVP antibodies. The MVP immunoblot was re-probed for SHP-2. *C*, cell lysates from the above experiment were immunoblotted with anti-MVP, anti-SHP-2, anti-phospho-Erk, and anti-Erk2 antibodies. *D*, the resultant GST affinity precipitates of GST-SHP-2 full-length (GST-SHP-2-FL) and tandem SH2 domains of SHP-2 (GST-N+C-SH2) from lysates prepared from pervanadate-treated WI38 fibroblasts were immunoblotted with anti-MVP antibodies. *E*, 293 cells were transfected with MVP-FLAG and serum-deprived for 24 h prior to stimulation with EGF (20 ng/ml) for 30 min. Affinity precipitates derived from GST and GST-N+C SH2 domains from unstimulated and EGF (20 ng/ml) stimulated 293 cells were resolved by 8% SDS-PAGE and immunoblotted with anti-FLAG antibodies. *F*, WI38 fibroblasts were serum-deprived for 24 h and were either left unstimulated (*Untreated*) or were stimulated with EGF (100 ng/ml) for 90 min (*EGF*). Confocal images for SHP-2 (*upper panel*) and MVP (*middle panel*) and merged images for both (*lower panel*) under untreated and EGF-stimulated conditions are shown. Co-localization between SHP-2 and MVP (yellow) is observed under EGF-stimulated conditions in the cytoplasm but not in the nucleus.

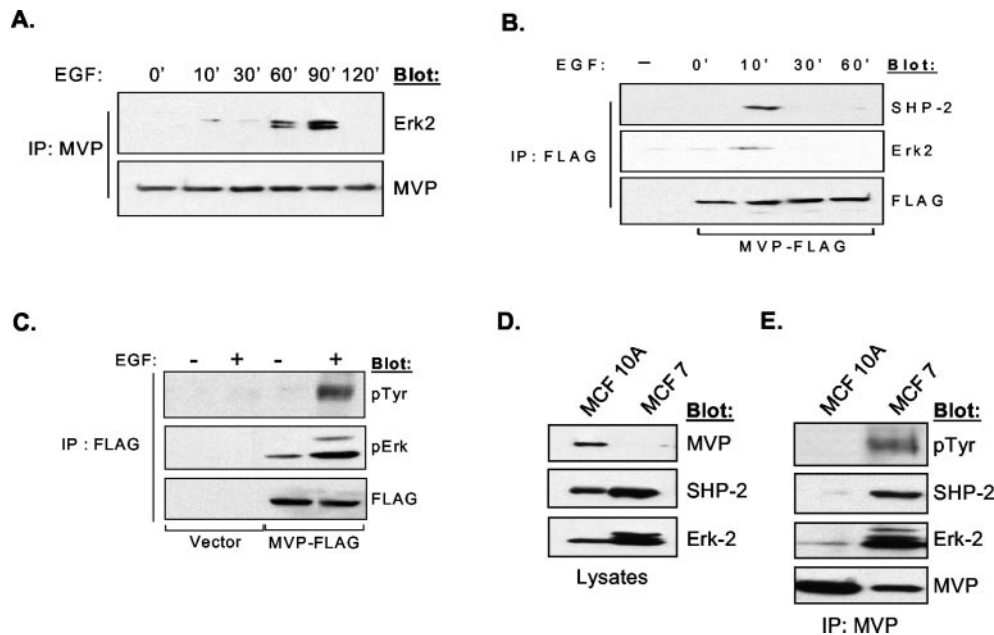


FIG. 5. Tyrosyl-phosphorylated MVP interacts with activated Erk2. *A*, serum-deprived and EGF-stimulated WI38 cell lysates were immunoprecipitated with anti-MVP antibodies and immunoblotted for Erk2. The *lower panel* shows the re-probe for MVP. *B*, 293 cells were transfected with MVP-FLAG as indicated. MVP was immunoprecipitated with anti-FLAG antibodies and immunoblotted for SHP-2 and Erk2 from lysates prepared from serum-deprived and EGF-stimulated 293 cell transfectants. The *lower panel* represents the re-probe for MVP-FLAG. *C*, 293 cells transfected with either vector or MVP-FLAG were serum-deprived for 24 h and either left unstimulated or stimulated with EGF (20 ng/ml). MVP-FLAG was immunoprecipitated with anti-FLAG antibodies and immunoblotted with anti-phosphotyrosine antibodies (*upper panel*) and anti-phospho-Erk (*middle panel*) antibodies and re-probed for MVP-FLAG (*lower panel*). *D*, lysates from serum-deprived MCF-10A and MCF-7 cells were immunoblotted with anti-MVP, anti-SHP-2, and anti-Erk2 antibodies. *E*, MVP was immunoprecipitated from lysates that were generated from serum-deprived MCF-10A and MCF-7 cells. Anti-MVP immune complexes were immunoblotted for phosphotyrosine (pTyr), SHP-2, Erk2, and MVP as indicated.

lowing EGF stimulation, the amount of the activated form of Erk bound to MVP was greatly enhanced (Fig. 5C). These observations imply that in response to EGF, MVP tyrosyl phosphorylation promotes the interaction with the activated form of the Erks.

We also compared the tyrosyl phosphorylation status of MVP and its ability to associate with both SHP-2 and Erk in spontaneously immortalized normal breast epithelial (MCF-10A) and in breast cancer cells (MCF-7). MVP was immunoprecipitated from lysates (Fig. 5D) derived from serum-deprived MCF-10A and MCF-7 cells, and the immune complexes were immunoblotted with anti-phosphotyrosine antibodies. MVP was found to be hyper-tyrosyl-phosphorylated in MCF-7 cells as compared with normal MCF-10A cells, despite the fact that less MVP was recovered from lysates derived from MCF-7 cells as compared with MCF-10A cells (Fig. 5, D and E). Moreover, MVP was constitutively associated with both SHP-2 and Erk2 in MCF-7 cells, whereas these interactions were barely detectable in MCF-10A cells (Fig. 5E). In context of the data presented in Fig. 4, these data suggest that the association of both SHP-2 and Erk2 with MVP is dependent upon MVP tyrosyl phosphorylation.

Effect of EGF-mediated Erk and Elk-1 Activation in MVP-deficient MEFs—SHP-2 positively regulates EGF-mediated activation of Erk and Elk-1 in response to EGF (37). Because MVP was found to interact with both SHP-2 and Erk, we hypothesized that it may participate in EGF-dependent activation of Erk and subsequently Elk-1. To determine whether MVP is involved in EGF-dependent signaling to Erk and Elk-1, we utilized wild type (MVP^{+/+}) and MVP-deficient (MVP^{-/-}) MEFs. MVP^{-/-} MEFs derived from mice containing a homozygous deletion for MVP (34) lacked MVP expression, whereas in MVP^{+/+} MEFs the expression of MVP was readily detected (Fig. 6A). MVP^{+/+} and MVP^{-/-} MEFs were serum-deprived for 24 h and then re-stimulated with EGF for varying times. Cell lysates prepared from these MEFs were immunoblotted for the

detection of activated Erk using anti-phospho-Erk antibodies. No dramatic differences in the overall activation of the Erks between MVP^{+/+} and MVP^{-/-} MEFs in response to EGF stimulation were observed (Fig. 6A). However, more subtle changes in the kinetics of Erk activation were noted (Fig. 6A). We consistently observed that in MVP^{-/-} MEFs maximal Erk activation was delayed within the first 5 min following EGF stimulation but was more sustained later on, as compared with MVP^{+/+} MEFs (Fig. 6A).

We next sought to determine whether MVP affects the activation of Elk-1 in response to EGF. MVP^{+/+} and MVP^{-/-} MEFs were transfected with Elk-Gal4 along with 5X-Gal4-luciferase. Cells were serum-deprived for 24 h, then stimulated with EGF for 4 h and assayed for Elk-mediated luciferase activity. Fig. 6B shows that in MVP^{-/-} MEFs, basal Elk-1 transactivation was reduced by ~50% as compared with MVP^{+/+} MEFs. In response to EGF stimulation, MVP^{-/-} MEFs were still capable of activating Elk-1; however, the magnitude of this activation was significantly lower than MVP^{+/+} MEFs (Fig. 6B). In contrast, when MVP-FLAG was transfected into 293 cells an enhanced level of basal, and a significantly elevated level of Elk-1 transactivation following EGF stimulation, as compared with vector control transfected 293 cells was observed (Fig. 6C). Next, we determined whether the defect in EGF-induced Elk-1 activation in MVP^{-/-} MEFs could be rescued by a gain-of-function mutant of Ras. An activated Ras(V12) mutant was transiently transfected into MVP^{+/+} and MVP^{-/-} MEFs in the absence of growth factors and Elk-1-mediated luciferase activity measured. Again, basal Elk-1 activity was lower in MVP^{-/-} MEFs as compared with MVP^{+/+} MEFs (Fig. 6D). However, the activation of Elk-1 in Ras(V12)-transfected MVP^{-/-} MEFs was significantly lower than in MVP^{+/+} MEFs (Fig. 6D). These data suggest that MVP can suppress the effects of Ras(V12) suggesting that MVP functions either downstream of, and/or parallel to, Ras in the activation of Elk-1.

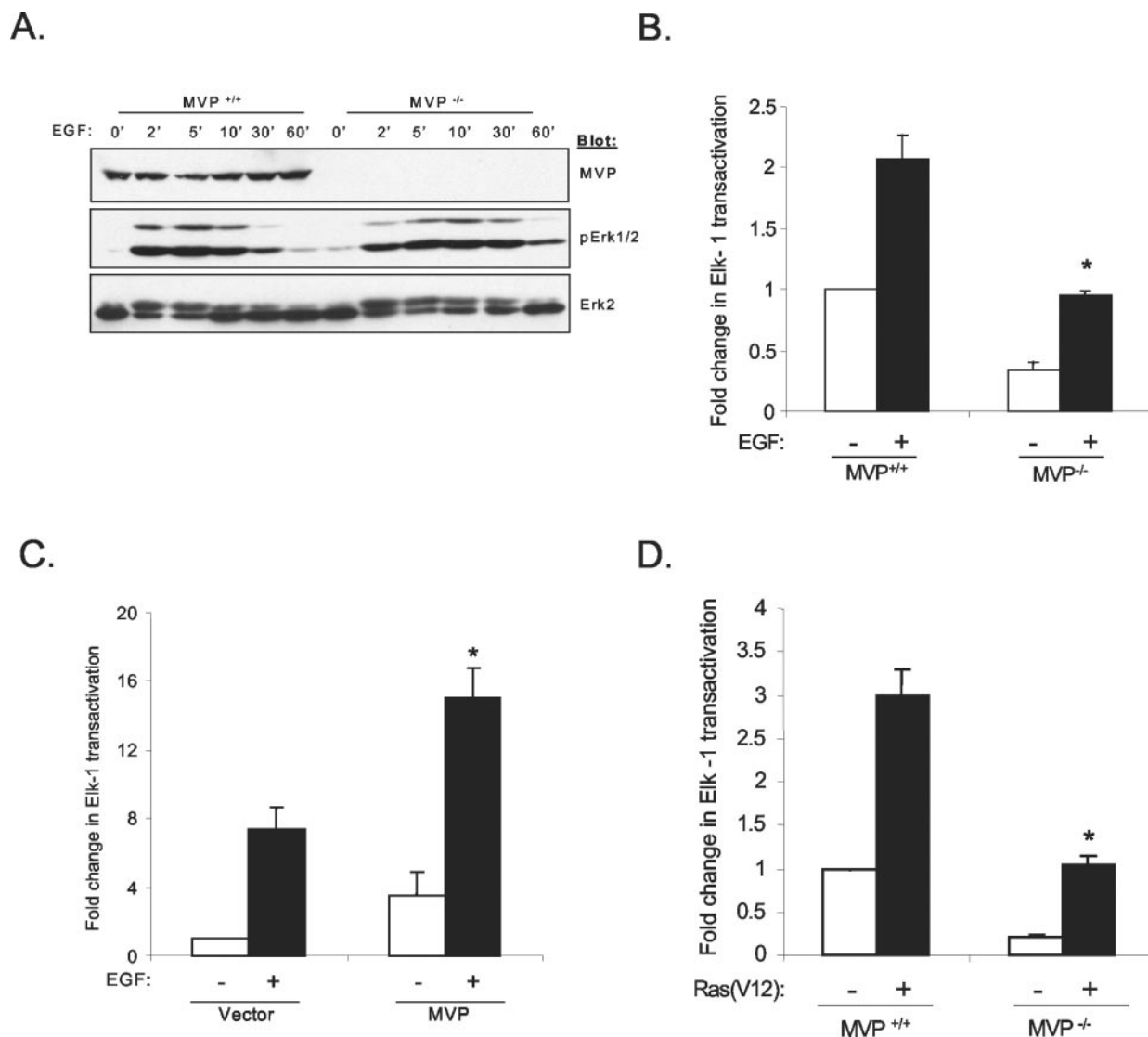


FIG. 6. Effect of EGF-mediated Erk and Elk-1 activation in MVP-deficient MEFs. A, MVP^{+/+} and MVP^{-/-} MEFs were serum-deprived for 24 h prior to stimulation with EGF (100 ng/ml) for different time periods. Lysates prepared from these cells were resolved on 8% SDS-PAGE and immunoblotted for MVP (upper panel), phospho-Erk1/2 (middle panel), and Erk2 (lower panel) using polyclonal anti-MVP, anti-phospho-Erk1/2, and anti-Erk2 antibodies, respectively. B, MVP^{+/+} and MVP^{-/-} MEFs transfected with Elk1 and 5X-Gal4-luc reporter along with *Renilla* were serum-deprived for 24 h and stimulated with EGF (100 ng/ml) for 4 h. Transfections were performed in triplicate, and the Elk-1 luciferase activities were normalized to *Renilla*. Data are representative of the mean \pm S.E. from four independent experiments (*, $p < 0.05$). C, either vector or MVP-FLAG was expressed in 293 cells that were stimulated with EGF and assayed for luciferase activity as described for B. Data represent the mean \pm S.E. of four independent experiments performed in triplicate (*, $p < 0.05$). D, MVP^{+/+} and MVP^{-/-} fibroblasts co-transfected with Ras(V12) were serum-deprived for 24 h and assayed for luciferase activity as described for B. Data represent the mean \pm S.E. of three independent experiments performed in triplicates (*, $p < 0.05$).

MVP Is Required for Cell Survival—MVP has been suggested to be involved in drug resistance in cancer cells (32). We therefore compared the ability of MVP^{+/+} and MVP^{-/-} MEFs to either proliferate in response to serum or to survive following growth factor withdrawal. In response to either 10, 5, or 2.5% serum we found that MVP^{+/+} and MVP^{-/-} MEFs were equivalent in their proliferation rates (data not shown). However, when serum-deprived for 24 h, MVP^{-/-} MEFs showed significantly increased levels of cell death than MVP^{+/+} MEFs, as measured by either the percentage of trypan blue excluded MEFs (Fig. 7A) or by FACS analysis for detection of the sub-G₀/G₁ population (Fig. 7B). These data demonstrate that MVP is required for cell survival in response to growth factor deprivation.

DISCUSSION

SHP-2 has been implicated in a variety of cellular processes (9, 10). However, the mechanisms for how SHP-2 regulates cell

signaling have not been clarified completely because its physiological substrates still remain to be identified. We present evidence that supports the conclusion that MVP is a novel substrate for SHP-2. We show that MVP complexes with SHP-2 via a mechanism that involves the substrate-trapping mutant of SHP-2 (Figs. 1–3). Another criterion used in defining PTP substrates is that the substrate can be dephosphorylated by the PTP directly. We show that both the activated mutant of SHP-2 and the PTP domain alone dephosphorylated MVP *in vitro*, and this dephosphorylation was inhibited by vanadate (Fig. 2). Although the activated SHP-2 assumes an open/active conformation and exhibits levels of phosphatase activity equivalent to that of the PTP domain alone, it only partially dephosphorylated MVP (Fig. 2B). These data suggest that in context of the full-length activated SHP-2, there exists some level of substrate specificity for a subset of MVP phosphotyrosyl residues. In fact, there is precedence for such site specific dephosphoryl-

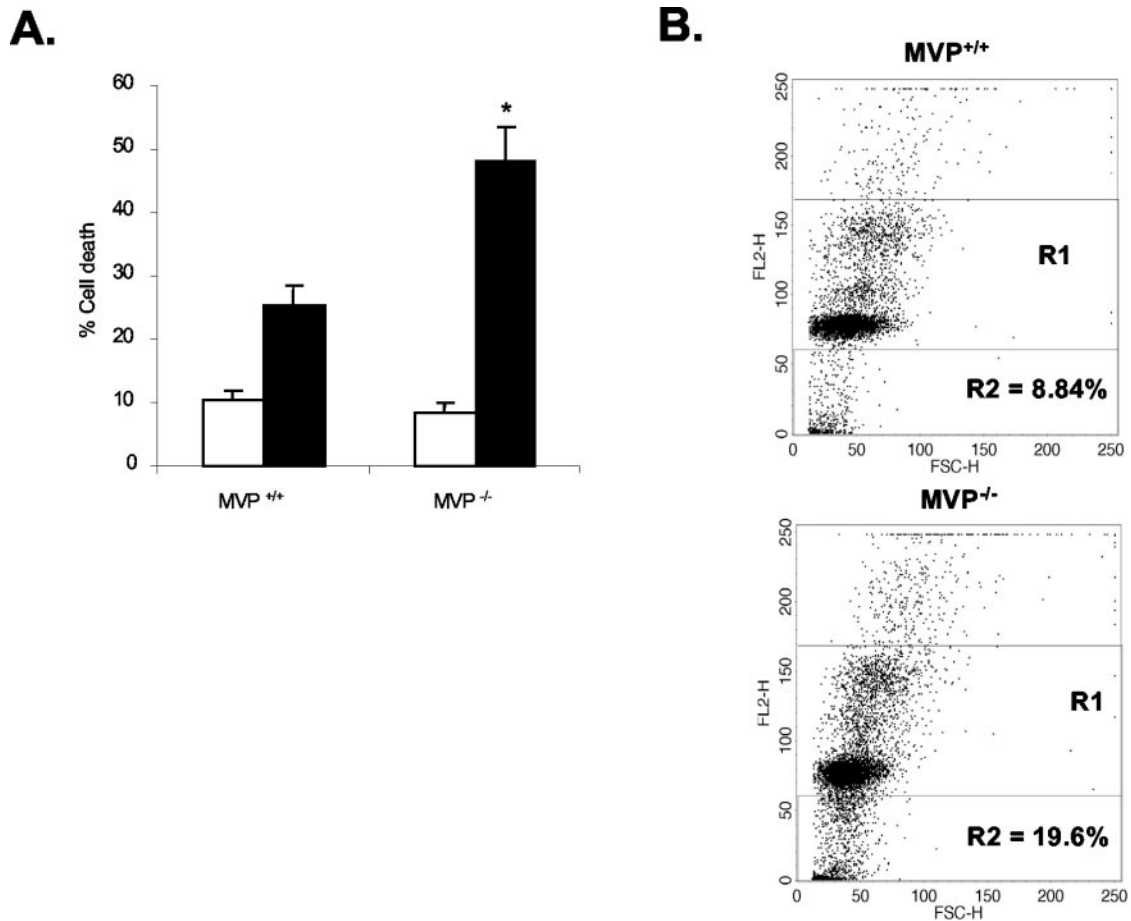


FIG. 7. MVP is required for cell survival. A, MVP^{+/+} and MVP^{-/-} MEFs were either cultured in the presence of 10% serum (□) or were serum-deprived for 24 h (■). The percentage of trypan blue-positive cells from the total population of both non-adherent and adherent MEFs were counted. Data represent the mean ± S.E. of three independent experiments performed in duplicate (*, *p* < 0.05). B, MVP^{+/+} and MVP^{-/-} MEFs treated as described above were stained with propidium iodide, and cell death was analyzed by quantitating the sub-G₀/G₁ population of cells (R2) by FACS analysis. These data are representative of three separate experiments performed in duplicate.

ation by SHP-2 as seen on Tyr⁷⁷¹ of the platelet-derived growth factor receptor (44), the phosphatidylinositol 3-kinase binding site on Gab-1 (12), and the EGF receptor (27).

We also demonstrate that MVP interacts with full-length SHP-2 in a substrate-trapping manner *in vivo* in quiescent cells (Fig. 3C). These data argue that the site of SHP-2 tyrosyl dephosphorylation on MVP exists prior to growth factor stimulation. This is consistent with the purification strategy designed to isolate substrates of SHP-2 that were tyrosyl-phosphorylated prior to receptor activation (Fig. 1). It is intriguing that upon EGF stimulation, the SHP-2 substrate-trapped MVP complex dissociated. It is conceivable that further tyrosine, serine, or threonine phosphorylation and/or dephosphorylation of MVP following EGF stimulation disrupts the enzyme-substrate complex between SHP-2 and MVP. The precise reason for this dissociation, however, is unclear.

Many enzymes interact with their substrates, in a catalytic-site independent manner, to facilitate catalysis. Consistent with this, MVP was found to associate with SHP-2 basally. Upon EGF stimulation, this interaction was enhanced in a manner that correlated with increased MVP tyrosyl phosphorylation levels (Fig. 4). Together, these observations are consistent with the model that SHP-2 interacts with MVP via its SH2 domains thereby facilitating the ability of SHP-2 to dephosphorylate MVP, as well as to initiate signaling events by either dephosphorylating MVP itself and/or other targets that may be within proximity to the MVP complex (Fig. 8). Thus, MVP behaves in a similar manner to other known SHP-2

scaffold proteins such as those of the IRS, Gab, and FRS families in which tyrosyl phosphorylation of these scaffold proteins serves to recruit and activate SHP-2 (10).

We have discovered that MVP interacts with Erk2 in response to EGF, either when overexpressed in 293 cells or endogenously in WI38 fibroblasts. Significantly, activated Erk was bound to MVP following EGF stimulation (Fig. 5C). These data suggest the possibility that EGF-induced tyrosyl phosphorylation of MVP promotes the assembly with activated Erk. In support of this, we demonstrated that in MCF-7 cells in which MVP is heavily tyrosyl-phosphorylated, a complex between MVP, Erk, and SHP-2 is detected. In contrast, such a complex is not detected in MCF-10A cells where MVP is not detectably tyrosyl-phosphorylated (Fig. 5E). Thus, we provide the first evidence to suggest that MVP functions as a *bona fide* signaling scaffold for the Erk pathway.

SHP-2 is known to positively regulate EGF-mediated activation of the Erk pathway (37). We therefore tested whether MVP also is involved in regulating signaling through the EGF receptor. We found that MVP-deficient MEFs were responsive to EGF-induced Erk activation to levels equivalent to that of wild type MEFs. Nevertheless, we did observe more subtle but consistent differences in the kinetics of Erk activation in response to EGF between wild type and MVP-deficient MEFs (Fig. 6A). These observations suggest that MVP might play more of a modulatory role in Erk activation rather than a stimulatory and/or inhibitory one. The idea that MVP may function to “fine-tune” the kinetics of Erk activity is reminiscent of the

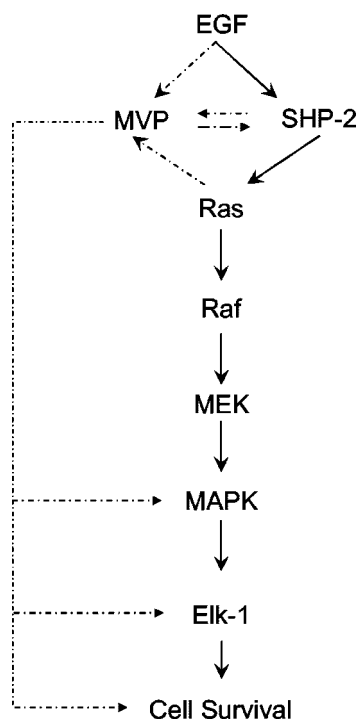


FIG. 8. **Model for SHP-2 regulation of MVP tyrosyl phosphorylation in EGF-mediated signaling.** Solid arrows show established signaling pathways and broken arrows indicate potential signaling pathways proposed in this work. Upon EGF stimulation, MVP becomes tyrosyl-phosphorylated and recruits SHP-2 leading to MVP tyrosyl dephosphorylation. SHP-2 may also signal downstream to Ras from MVP once activated. MVP interacts with Erk and cooperates with Ras to provide optimal activation of Elk-1 in response to EGF leading either directly or indirectly to the regulation of cell survival.

actions of scaffold proteins such as KSR (45), MP-1 (46), and CNK (47), which are thought to act as signal facilitators rather than critical components required for signal initiation.

Given that MVP-deficient MEFs exhibited only subtle differences in the activation of Erk in response to EGF, we were surprised to find that the activity of the ternary complex factor Elk-1, which is an Erk substrate, was significantly inhibited in MVP-deficient fibroblasts (Fig. 6B). In addition, overexpression of MVP in 293 cells potentiated EGF-induced Elk-1 activation (Fig. 6C). Elk-1 phosphorylation by Erk, as well as other MAPKs, is necessary but not sufficient for its activation (48). Thus, although Erk activity is largely unaffected in MVP-deficient MEFs, these data demonstrate that MVP participates in a signaling pathway to regulate Elk-1 activity. It is conceivable that MVP is required for the activation of other MAPKs involved in stimulating Elk-1 such as the c-Jun NH₂-terminal kinase (JNK) and/or p38 MAPK. However, we find that stimulation of 293 cells with EGF results only in the activation of Erk,² suggesting that Erk, rather than JNK and/or p38 MAPK, participates in promoting Elk-1 activation when MVP is overexpressed. The finding that MVP controls a signaling pathway that mediates Elk-1 activation independently of the Erks has also been demonstrated for other adaptor/scaffold proteins such as KSR, Gab-2, IRS-1, and intersectin (16, 49–51).

An interesting finding in this study is the ability of MVP to suppress the activity of Elk-1 by a constitutively active mutant of Ras (Fig. 6D). These data suggest that MVP functions downstream of and/or parallel to Ras. Provocatively, there is again a striking similarity between the signaling properties of MVP and those exhibited by KSR. Like MVP, KSR can also suppress

the phenotype of a constitutively active mutant of Ras (52–54). We hypothesize that MVP tyrosyl phosphorylation, which promotes the binding and subsequent activation of SHP-2, may serve to initiate a signaling cascade that cooperates with Ras in the regulation of Elk-1 (Fig. 8). The idea that MVP may function in growth factor signal transduction is indirectly supported by the observation that disruption of vaults in *Dictyostelium* results in growth and morphological defects under nutrient stress (55). Taken together, our data now demonstrate in mammalian systems that MVP is integrally regulated at the level of tyrosyl phosphorylation by the EGF receptor pathway, and it is directly involved in modulating signaling effects from this receptor in the control of gene expression (Fig. 8).

Recent studies using MVP knock-out mice demonstrate that MVP is dispensable for development (34). Although MVP has been proposed to play a role in drug resistance (32), MVP knock-out mice fail to exhibit any enhanced sensitivity to drug-induced apoptosis (34). Overexpression of MVP has been correlated with multidrug resistance in various chemoresistant tumors such as small cell and non-small cell lung cancers, breast, colon, ovarian carcinomas, and glioblastomas to name a few (30, 31). Using MVP-deficient MEFs, we have made the exciting finding that MVP is involved in supporting cell survival, since MVP-deficient MEFs undergo significantly enhanced levels of cell death following growth factor withdrawal as compared with wild type MEFs (Fig. 7). These data provide a functional role for MVP in cell survival. We have recently shown that SHP-2 is also involved in cell survival and apoptosis by controlling the activity of the insulin-like growth factor/phosphatidylinositol 3-kinase/Akt pathway (13). In this regard, we have found that MVP also becomes tyrosyl-phosphorylated in response to IGF-1.³ It is reasonable to speculate that MVP tyrosyl phosphorylation may promote the recruitment and subsequent activation of SHP-2 in response to IGF-1 leading to the engagement of the Akt survival pathway.

Our data may also begin to resolve some of the controversy regarding the nature of the predictive value of MVP expression levels as an indicator of chemoresponsiveness (56–59). Perhaps, the tyrosyl phosphorylation status of MVP, and subsequently its ability to recruit and activate SHP-2, is a more relevant correlate with drug resistance rather than the levels of MVP protein expression. The regulation of MVP tyrosyl phosphorylation by SHP-2 at specific phosphotyrosyl residues on MVP may either positively or negatively regulate the ability of MVP to associate with signaling molecules, such as Erk2, that participate in transducing survival signals. We propose that the regulation of MVP tyrosyl phosphorylation by SHP-2 plays an important role in the modulation of growth factor signaling. These data raise new possibilities into how MVP may function in drug resistance and possibly cancer progression.

Acknowledgments—We thank Dr. Nigel Ewing for performing the MALDI-TOF analyses, Matteus Guerra for assistance with confocal microscopy, and Dr. Paul Lombroso for comments on the manuscript.

REFERENCES

- Feng, G.-S., Hui, C.-C., and Pawson, T. (1993) *Science* **259**, 1607–1611
- Freeman, R. M., Plutzky, J., and Neel, B. G. (1992) *Proc. Natl. Acad. Sci. U. S. A.* **89**, 11239–11243
- Vogel, W., Lammers, R., Huang, J., and Ullrich, A. (1993) *Science* **259**, 1611–1614
- Van Vactor, D., O'Reilly, A. M., and Neel, B. G. (1998) *Curr. Opin. Genet. Dev.* **8**, 112–126
- Saxton, T. M., Henkemeyer, M., Gasca, S., Shen, R., Rossi, D. J., Shalaby, F., Feng, G. S., and Pawson, T. (1997) *EMBO J.* **16**, 2352–2364
- Oh, E. S., Gu, H., Saxton, T. M., Timms, J. F., Hausdorff, S., Frevert, E. U., Kahn, B. B., Pawson, T., Neel, B. G., and Thomas, S. M. (1999) *Mol. Cell. Biol.* **19**, 3205–3215
- Shi, Z. Q., Lu, W., and Feng, G. S. (1998) *J. Biol. Chem.* **273**, 4904–4908

² J. J. Wu and A. M. Bennett, unpublished observations.

³ S. Kolli and A. M. Bennett, unpublished observations.

8. Wu, C. J., O'Rourke, D. M., Feng, G. S., Johnson, G. R., Wang, Q., and Greene, M. I. (2001) *Oncogene* **20**, 6018–6025
9. Feng, G. S. (1999) *Exp. Cell Res.* **253**, 47–54
10. Neel, B. G., Gu, H., and Pao, L. (2003) *Trends Biochem. Sci.* **28**, 284–293
11. Noguchi, T., Matozaki, T., Horita, K., Fujioka, Y., and Kasuga, M. (1994) *Mol. Cell. Biol.* **14**, 6674–6682
12. Zhang, S. Q., Tsiaras, W. G., Araki, T., Wen, G., Minichiello, L., Klein, R., and Neel, B. G. (2002) *Mol. Cell. Biol.* **22**, 4062–4072
13. Zito, C. I., Kontaridis, M. I., Fornaro, M., Feng, G. S., and Bennett, A. M. (2004) *J. Cell. Physiol.* **199**, 227–236
14. Walter, A. O., Peng, Z. Y., and Cartwright, C. A. (1999) *Oncogene* **18**, 1911–1920
15. Zhang, S. Q., Yang, W., Kontaridis, M. I., Bivona, T. G., Wen, G., Araki, T., Luo, J., Thompson, J. A., Schraven, B. L., Philips, M. R., and Neel, B. G. (2004) *Mol. Cell* **13**, 341–355
16. Gu, H., Pratt, J. C., Burakoff, S. J., and Neel, B. G. (1998) *Mol. Cell* **2**, 729–740
17. Holgado-Madruga, M., Emlet, D. R., Moscatello, D. K., Godwin, A. K., and Wong, A. J. (1996) *Nature* **379**, 560–564
18. Kouhara, H., Hadari, Y. R., Spivak-Kroizman, T., Schilling, J., Bar-Sagi, D., Lax, I., and Schlessinger, J. (1997) *Cell* **89**, 693–702
19. Kuhné, M. R., Pawson, T., Lienhard, G. V., and Feng, G.-S. (1993) *J. Biol. Chem.* **268**, 11479–11481
20. Fujioka, Y., Matozaki, T., Noguchi, T., Iwamatsu, A., Yamao, T., Takahashi, N., Tsuda, M., Takada, T., and Kasuga, M. (1996) *Mol. Cell. Biol.* **16**, 6887–6899
21. Jackson, D. E., Ward, C. M., Wang, R., and Newman, P. J. (1997) *J. Biol. Chem.* **272**, 6986–6993
22. Zhao, Z. J., and Zhao, R. (1998) *J. Biol. Chem.* **273**, 29367–29372
23. Barford, D., and Neel, B. G. (1998) *Structure (Lond.)* **6**, 249–254
24. Agazie, Y. M., and Hayman, M. J. (2003) *J. Biol. Chem.* **278**, 13952–13958
25. Wu, T. R., Hong, Y. K., Wang, X. D., Ling, M. Y., Dragoi, A. M., Chung, A. S., Campbell, A. G., Han, Z. Y., Feng, G. S., and Chin, Y. E. (2002) *J. Biol. Chem.* **277**, 47572–47580
26. Yu, C. L., Jin, Y. J., and Burakoff, S. J. (2000) *J. Biol. Chem.* **275**, 599–604
27. Agazie, Y. M., and Hayman, M. J. (2003) *Mol. Cell. Biol.* **23**, 7875–7886
28. Kontaridis, M. I., Eminaga, S., Fornaro, M., Zito, C. I., Sordella, R., Settleman, J., and Bennett, A. M. (2004) *Mol. Cell. Biol.* **24**, 5340–5352
29. Scheffer, G. L., Wijngaard, P. L., Flens, M. J., Izquierdo, M. A., Slovak, M. L., Pinedo, H. M., Meijer, C. J., Clevers, H. C., and Scheper, R. J. (1995) *Nat. Med.* **1**, 578–582
30. Suprenant, K. A. (2002) *Biochemistry* **41**, 14447–14454
31. Scheffer, G. L., Schroeijers, A. B., Izquierdo, M. A., Wiemer, E. A., and Scheper, R. J. (2000) *Curr. Opin. Oncol.* **12**, 550–556
32. Mossink, M. H., van Zon, A., Scheper, R. J., Sonneveld, P., and Wiemer, E. A. (2003) *Oncogene* **22**, 7458–7467
33. Kolli, S., Buchmann, A. M., Williams, J., Weitzman, S., and Thimmapaya, B. (2001) *Proc. Natl. Acad. Sci. U. S. A.* **98**, 4646–4651
34. Mossink, M. H., van Zon, A., Franzel-Luiten, E., Schoester, M., Kickhoefer, V. A., Scheffer, G. L., Scheper, R. J., Sonneveld, P., and Wiemer, E. A. (2002) *Cancer Res.* **62**, 7298–7304
35. Kontaridis, M. I., Liu, X., Zhang, L., and Bennett, A. M. (2002) *Mol. Cell. Biol.* **22**, 3875–3891
36. Hausdorff, S. F., Bennett, A. M., Neel, B. G., and Birnbaum, M. J. (1995) *J. Biol. Chem.* **270**, 12965–12968
37. Bennett, A. M., Hausdorff, S. F., O'Reilly, A. M., Freeman, R. M., and Neel, B. G. (1996) *Mol. Cell. Biol.* **16**, 1189–1202
38. Pusl, T., Wu, J. J., Zimmerman, T. L., Zhang, L., Ehrlich, B. E., Berchtold, M. W., Hoek, J. B., Karpen, S. J., Nathanson, M. H., and Bennett, A. M. (2002) *J. Biol. Chem.* **277**, 27517–27527
39. Herrmann, C., Volknandt, W., Wittich, B., Kellner, R., and Zimmermann, H. (1996) *J. Biol. Chem.* **271**, 13908–13915
40. O'Reilly, A., Pluskey, S., Shoelson, S. E., and Neel, B. G. (2000) *Mol. Cell. Biol.* **20**, 299–311
41. van Zon, A., Mossink, M. H., Schoester, M., Scheffer, G. L., Scheper, R. J., Sonneveld, P., and Wiemer, E. A. (2001) *J. Biol. Chem.* **276**, 37715–37721
42. Yuan, L., Yu, W.-M., Yuan, Z., Haudenschild, C. C., and Qu, C.-K. (2003) *J. Biol. Chem.* **278**, 15208–15216
43. Chugani, D., Rome, L., and Kedersha, N. (1993) *J. Cell Sci.* **106**, 23–29
44. Klinghoffer, R. A., and Kazlauskas, A. (1995) *J. Biol. Chem.* **270**, 22208–22217
45. Morrison, D. K. (2001) *J. Cell Sci.* **114**, 1609–1612
46. Schaeffer, H. J., Catling, A. D., Eblen, X. T., Collier, L. A., Krauss, A., and Weber, M. J. (1998) *Science* **281**, 1668–1671
47. Therrien, M., Wong, A. M., and Rubin, G. M. (1998) *Cell* **95**, 343–353
48. Yang, S.-H., Sharrocks, A. D., and Whitmarsh, A. J. (2003) *Gene (Amst.)* **320**, 3–21
49. Sugimoto, T., Stewart, S., Han, M., and Guan, K.-L. (1998) *EMBO J.* **17**, 1717–1727
50. Bruning, J., Winnay, J., Cheatham, B., and Kahn, C. (1997) *Mol. Cell. Biol.* **17**, 1513–1521
51. Adams, A., Thorn, J. M., Yamabhai, M., Kay, B. K., and O'Bryan, J. P. (2000) *J. Biol. Chem.* **275**, 27414–27420
52. Therrien, M., Chang, H. C., Solomon, N. M., Karim, F. D., Wassarman, D. A., and Rubin, G. M. (1995) *Cell* **83**, 879–888
53. Sundaram, M., and Han, M. (1995) *Cell* **83**, 889–901
54. Kornfeld, K., Hom, D. B., and Horvitz, H. R. (1995) *Cell* **83**, 903–913
55. Vasu, S. K., and Rome, L. H. (1995) *J. Biol. Chem.* **270**, 16588–16594
56. Meijer, G. A., Schroeijers, A. B., Flens, M. J., Meuwissen, S. G., van der Valk, P., Baak, J. P., and Scheper, R. J. (1999) *J. Clin. Pathol.* **52**, 450–454
57. Uozaki, H., Horiuchi, H., Ishida, T., Iijima, T., Imamura, T., and Machinami, R. (1997) *Cancer* **79**, 2336–2344
58. Pohl, G., Filipits, M., Suchomel, R. W., Stranzl, T., Depisch, D., and Pirker, R. (1999) *Anticancer Res.* **19**, 5051–5055
59. Linn, S. C., Pinedo, H. M., van Ark-Otte, J., van der Valk, P., Hoekman, K., Honkoop, A. H., Vermorcken, J. B., and Giaccone, G. (1997) *Int. J. Cancer* **71**, 787–795